Available online at www.sciencedirect.com

ScienceDirect

Procedia Computer Science 119 (2017) 245–254

Procedia Computer Science

www.elsevier.com/locate/procedia

6th International Young Scientists Conference in HPC and Simulation, YSC 2017, 1-3 November 2017, Kotka, Finland

Simulation of Overdrive Pacing in 2D Phenomenological Models of Anisotropic Myocardium

Timofei Epanchintsev[a,b,*], Sergei Pravdin[a,b], Andrey Sozykin[a,b], Alexander Panfilov[c]

[a] *Krasovskii Institute of Mathematics and Mechanics, Ekaterinburg, 620990, Russia*
[b] *Ural Federal University, Ekaterinburg, 620002, Russia*
[c] *Ghent University, Ghent, 9000, Belgium*

Abstract

Spiral waves in the heart underlie dangerous cardiac arrhythmias such as fibrillation. Low-voltage defibrillation and cardioversion are modern methods to treat such pathologies. This type of electrotherapy is based on the phenomenon of superseding spiral waves by a high-frequency source of excitation. In this paper, we numerically simulated the superseding process in a thin layer of the cardiac muscle. We captured the case of a sole spiral wave with a stable core at the centre of a square. We used different cell-level models as well as a variety of electrode configurations and studied the induced drift of the spiral wave. Regimes of the external stimulation were classified based on whether they provide an effective and safe, that is without break-up, way to shift the spiral toward the boundary.

Peer-review under responsibility of the scientific committee of the 6th International Young Scientist conference in HPC and Simulation

Keywords: heart simulation, defibrillation, cardioversion, myocardium, spiral wave, anisotropy, excitable medium
PACS: 87.19.Hh, 87.19.Nn
2010 MSC: 92C05

1. Introduction

Auto-wave processes are widely spread in nature and are an important focus of research in recent decades. Without an excitation source, auto-waves can disappear or be self-sustained. The sources of self-sustained auto-wave activity in excitable media may have the form of rotating spirals, called spiral waves. Such waves have been detected in excitable media of a physical, chemical and biological nature, for example, in the Belousov–Zhabotinsky (BZ) reaction, CO oxidation on Pt catalyst, in morphogenesis of Protozoa organisms (amoebas Dictiostelium discoedeum), as well as in the retina, the nervous and cardiac tissue. Spiral waves underlie the mechanisms of several pathological conditions

* Corresponding author. Tel.: +7-343-362-8163.
E-mail address: eti@imm.uran.ru

1877-0509
Peer-review under responsibility of the scientific committee of the 6th International Young Scientist conference in HPC and Simulation
10.1016/j.procs.2017.11.182

with a great socio-economic impact, such as cardiac arrhythmias, migraines and, epilepsy. The appearance of spiral waves in the myocardium leads to paroxysmal tachycardia or fibrillation. These arrhythmias can affect the atria as well as the ventricles of the heart. In this regard, it is important to develop effective ways to control the dynamics and position of the spiral waves as it will result in development of better ways of managing these diseases. An effective method of treatment is electrical (high-voltage) cardioversion-defibrillation, though it is rather traumatic for myocardium and very stressful for the patient. Therefore an extremely important direction of research is finding new ways of removing spiral waves in the heart without utilizing high-voltage shocks. This topic of research is often regarded as low-voltage cardioversion-defibrillation (LVCD). This research is important for the development of implantable low-voltage cardioverters-defibrillators.

Numerical studies of LVCD were initiated using a two-variable model for cardiac tissue in [3], where a geometric explanation of the mechanism of drift was also proposed. Attempts to investigate LVCD theoretically and experimentally in the case of multiple spiral waves have been made (see for example [21, 9, 2]). There have been clinical studies of LVCD in case of paroxysmal tachycardia [19, 17], which showed an effectiveness of about 70%.

There are theoretical results of LVCD for a spiral wave rotating around an unexcitable heterogeneity (for example, a scar after a myocardial infarction) in a 2-dimensional medium model [16, 12]. In particular, it is shown that high-frequency stimulation cannot eliminate a wave rotating around an obstacle if its size is much larger than the size of the spiral wave core. Theoretical estimates of the maximal stimulation period necessary to eliminate the spiral wave were obtained. They depend on the radius of the circular obstacle and period of spiral wave rotation.

Another LVCD method is based on the effect of an external electric field on the entire myocardium. If spiral waves rotate around small unexcited or slowly-excitable regions, the external electric field can detach the wave from the obstacle and drive it to the border of the myocardium. This method was considered in works [9, 6, 20, 21, 2].

The case of the placement of a long flat electrode near the core of a spiral wave was analyzed theoretically, including a computational experiment [5]. Stimulation from an electrode located inside or near the core of the spiral wave was considered in [20].

Low-voltage superseding of stable (non-drifting without any external impact) spiral waves in myocardium was previously numerically studied in [14]. In that work, the myocardium was very simplistically modeled as an isotropic medium, and phenomenological cell-level models of Aliev–Panfilov (AP) [1] and a complex biophysical model of ion dynamics in cardiac cells TP06 [18] were used. It was shown that the spiral wave can react to external stimulation in three ways. First, it can be superseded and then disappear at the boundary. Second, the external stimulation can press the spiral to the boundary and cause the spiral to drift along the boundary or to stay near it. Third, break-up can occur. Effectiveness and safety of external stimulation was assessed. If model parameters are fixed, there is a segment of effective stimulation periods. Normally, a maximal effective stimulation period is slightly less than the spiral wave period. Stimulation periods close to the minimal effective limit can be unsafe due to break-up, whereas stimulation with periods close to the maximal effective limit requires maximal time to supersede the spiral. So, the stimulation seems to be effective and safe if its period is far enough from both limits.

Anisotropy is one of the main properties of the cardiac muscle, and the speed of the spread of electrical excitation is 2-4 times greater along the fibres than across them. The present work is devoted to studying LVCD in anisotropic myocardium models. We use the aforementioned phenomenological cell-level AP models and try broader limits of the stimulation period and more variants of electrode locations. After measuring the time of the beginning and ending of the spiral drift and determining the type of overall reaction of the spiral in the stimulation, we compare our findings with the results for the isotropic case. Due to the computational intensiveness of the task, we used a high-performance computer for our simulations.

2. Materials and Methods

In this Section, we present models of cardiac cells and tissue, protocols of stimulation, parameters of the models and a numerical method that we used. We also give details on our hardware and software as well as address its scalability index.

2.1. Electrophysiological Model

We used phenomenological dimensionless model AP [1] in two versions: APsimple and APmu. Propagation of wave excitation in the tissue was modelled using monodomain reaction-diffusion equations:

$$\frac{\partial u}{\partial t} = \operatorname{div}(D \operatorname{grad} u) + f(u, \vec{v}) + I_{\text{stim}}(\vec{r}, t), \qquad \frac{\partial \vec{v}}{\partial t} = \vec{g}(u, \vec{v}), \tag{1}$$

where $u = u(\vec{r}, t)$ is the transmembrane potential at the point $\vec{r} = (x, y)$ at the time t, $\vec{v} = \vec{v}(\vec{r}, t)$ is the vector of the other phase variables, $f(u, \vec{v})$ and $\vec{g}(u, \vec{v})$ are functions which depend on the cardiomyocyte model, $I_{\text{stim}}(\vec{r}, t)$ is the external stimulation current. To model anisotropic conduction along parallel cardiac myofibres, we used a uniaxially anisotropic diffusion tensor D with Cartesian components $D^{ij} = D_a\delta_{ij} + (D_f - D_a)\vec{w}^{\,i}\vec{w}^{\,j}$, $i, j = 1, 2$, where δ_{ij} is the Kronecker symbol and $\vec{w} = \vec{w}(\phi) = (\cos\phi, \sin\phi)$ is the unit vector of myofibre direction. Thereby, the diffusion coefficient is maximal and equal to D_f along $\vec{w}$, and is minimal and equal to D_a in the transverse direction. For the anisotropy, $D_f > D_a$, and for the isotropy, $D_f = D_a$.

At the medium boundaries, no-flux conditions $\vec{n} \cdot D \operatorname{grad} u = 0$ were imposed with the local normal vector $\vec{n}$.

In the case of APsimple model, system (1) has form:

$$\frac{\partial u}{\partial t} = \operatorname{div}(D \operatorname{grad} u) - ku(u - a)(u - 1) - uv + I_{\text{stim}}(x, y, t), \tag{2}$$

$$\frac{\partial v}{\partial t} = \epsilon(u)(ku - v), \qquad \text{where } \epsilon(u) = \begin{cases} 1, & \text{if } u < a; \\ \eta, & \text{otherwise.} \end{cases}$$

APmu model has the same equation (2) and the second equation in the following form:

$$\frac{\partial v}{\partial t} = -\left(\epsilon + \frac{\mu_1 v}{u + \mu_2}\right) \cdot (v + ku(u - a - 1)).$$

Stimulation current was equal I_{st} and was applied on region Ω_{stim} with period T_{stim} by impulses with duration t_{stim} starting from the moment τ_0:

$$I_{\text{stim}}(x, y, t) = \begin{cases} I_{\text{st}}, \text{ if } (x, y) \in \Omega_{\text{stim}},\ t \geqslant \tau_0,\ \left\{\frac{t-\tau_0}{T_{\text{stim}}}\right\} \leqslant \frac{t_{\text{stim}}}{T_{\text{stim}}}; \\ 0, \quad \text{otherwise.} \end{cases}$$

We found minimal value $I_{\min}$ of the current which caused action potential. Then we set $I_{\text{st}} := 4I_{\min}$. The stimulation was started when the spiral wave "controlled" the entire computational domain.

It is known that any spiral wave has a tip where its forefront and backfront meet. The spiral tip rotates around an area which is called the "core". A spiral wave is considered drifting if its core moves. Studying the dynamics of spiral waves is usually simplified by exploring the trajectory of the tip. To find it, we specified a certain level u^* of the

transmembrane potential, then the tip position $\vec{r}_{tip}$ was approximated by the following equations as was shown in [4]:

$$u(\vec{r}_{tip}, t) = u^*, \qquad u(\vec{r}_{tip}, t + \Delta t) = u^*,$$

where u^* and Δt are specific for each model. We set $u^* = 0.5$ for both AP models; $\Delta t = 2$ model units (MUs) for APsimple, 1 MU for APmu model (conversion coefficients for MU of time T and length L into ms and mm respectively are given below). The trajectory of the tip motion helps to determine the average drift velocity of the spiral wave and the type of its dynamics.

2.2. Computational Experiments

As electrical signals in the heart propagate faster along myofibres than across them, our model 2D square was anisotropic. We used dimensionless models so we provide parameters in MU. The diffusion coefficients were $D_f = 3$, $D_a = 0.3333$. The reaction-diffusion system was integrated using the finite difference and the explicit Euler methods with time step $dt = 0.008$ MU, space step $dr = 0.4$ MU, size of the mesh 160×160 MU.

S1S2 protocol [10] was used to make spiral waves. First, S1 stimulus induces a plane wave, which propagates from one side of a square to another. Then, S2 is given so that it crosses the backfront of the first plane wave. A spiral wave appears near the intersection. Stimulus S1 was applied to the left part of the square $x < 32$. Stimulus S2 was applied to the bottom half of the square $y < 80$ at the time 10 MU (44 MU) for APsimple (APmu).

External stimulation was launched from the electrode(s) after the spiral captured the entire computational space, so it started from $\tau_0 = 200$ MU.

Model APsimple had parameters $\eta = 0.1$, $a = 0.03, 0.04, \ldots, 0.1$.

Model APmu had only one parameter set: $k = 8$, $a = 0.1$, $\mu_1 = 0.2$, $\mu_2 = 0.3$, $\epsilon = 0.01$. It reproduces normal excitability of a healthy cardiomyocyte.

Parameter a is the most important parameter of the model and is responsible for excitability of cardiac tissue. The used range of parameter a covers all the reasonable values for excitability important for spiral wave dynamics [14]. The APmu parameter set is close to the parameter sets from the original papers [1, 11].

The stimulation current was 20 MU (3 MU) for APsimple (APmu); the external stimuli had a duration 0.1 MU (0.18 MU) for APsimple (APmu).

In Table 1, we give the temporal and spatial conversion coefficients from [14], where they were found using action potential duration APD-90, velocity of 1D waves and temporal periods of spiral waves for the both simple cardiomyocyte models and for the biophysical model TP06 [18].

Table 1. Parameters and characteristics of the myocardial models

Model, parameter a	APD-90, MU	T, ms	1D wave speed, MU	L, mm	Spiral wave period T_{sw}, MU
APsimple:					
$a = 0.03$	6.42	48	1.73	18.9	14.4
$a = 0.04$	6.27	49	1.66	20.0	14.6
$a = 0.05$	6.14	50	1.60	21.3	15.4
$a = 0.06$	6.00	51	1.53	22.7	17.2
$a = 0.07$	5.86	52	1.45	24.4	21.4
$a = 0.08$	5.74	53	1.37	26.3	30.8
$a = 0.09$	5.61	55	1.28	29.3	56
$a = 0.10$	5.49	56	1.16	32.7	184
APmu, $a = 0.1$	25.07	12.2	1.57	5.3	26

An important characteristic of a spiral wave is its temporal period T_{sw}. It is known that the period of the non-drifting wave is equal to the period of oscillations of the model phase variables outside the core of the spiral. We calculated the period of spiral waves as the time between the maxima of the transmembrane potential averaged by ten periods,

at a point outside the stimulation region and outside the core of the wave. We set the period of external stimulation relative to T_{sw}: $T_{stim} = P \cdot T_{sw}$ where $P = 0.7, 0.75, \ldots, 1.0$.

To take into account the interaction between fibre directions and boundary conditions, we conducted experiments with two directions of fibres: $\phi = 0$ and $\phi = \pi/4$. Spiral waves for these cases are shown in Fig. 1. Fibre direction is highlighted by black lines.

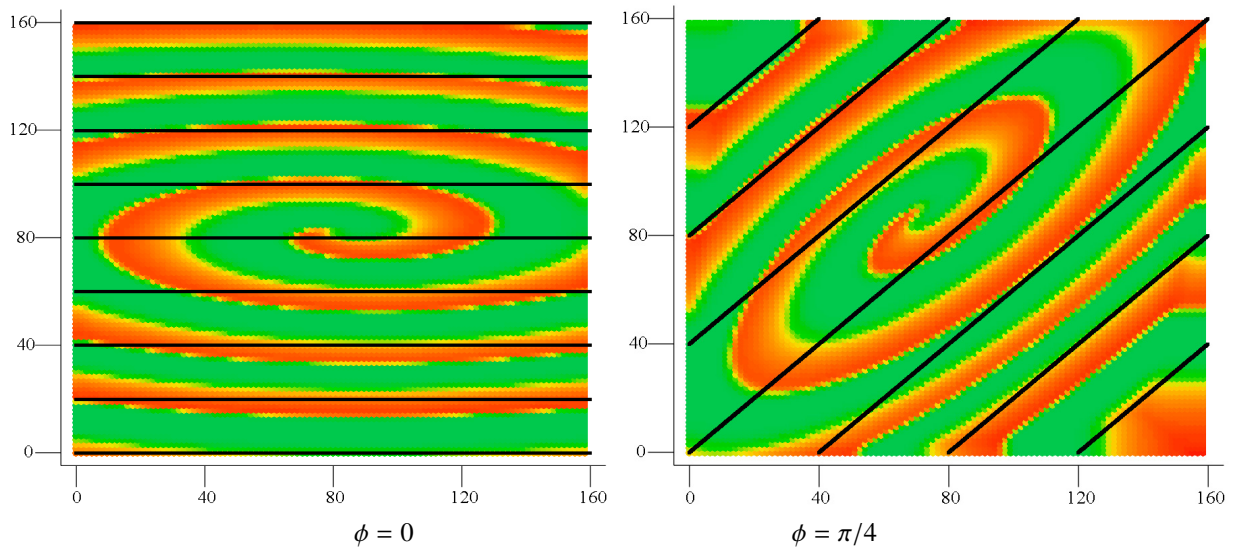

Fig. 1. Spiral waves and fibre directions, APmu model, $t = 180$ MU

We wrote our program in the C language (C99 version) and compiled using the Intel compiler icc. The most overloaded code sections were determined and accelerated using OpenMP, which decreased the simulation time significantly. We used a computational node whose configuration is presented in Table 2. The program has a nearly linear scalability (tested by simulation of 5000 MU of time with $\phi = \pi/4$ for both models, $a = 0.1$ for APsimple, and one stimulation electrode at the left bottom square corner). Table 3 shows simulation time with different number of cores. We achieved $\approx$ 16x time speedup on 32 cores. The simulation time for different cell models differed because APmu model gives slightly more computational load than APsimple.

All simulations were carried out on single node of *Uran* supercomputer of the Krasovskii Institute of Mathematics and Mechanics.

Table 2. Configuration of the computational node

CPU	6 x Intel(R) Xeon(R) CPU E5-2697 v4 @ 2.30GHz
RAM	252 GB
Operating System	CentOS 7.3

Table 3. The simulation time and achieved speedup using OpenMP

Number of cores	**1**	**2**	**4**	**8**	**16**	**32**
APsimple model						
Simulation time, sec	1296	657	359	198	124	81
Acceleration ratio	1	1.97	3.6	6.55	10.39	15.94
APmu model						
Simulation time, sec	1367	699	363	209	132	88
Acceleration ratio	1	1.95	3.76	6.54	10.35	15.49

3. Results

We use special designations for the spiral's response types.

A: spiral drifted from the electrode and disappeared at the boundary;
B: a drift to the boundary of the square, then along the boundary;
C: a drift to the boundary and stop;
D: no effect;
E: a spiral wave breakup;
AB: spiral drifted toward then along the boundary and finally disappeared;
Xn: *n* new spirals arose and disappeared whereas the main spiral's responce was X (X is A, B, C, D, or AB).

Fig. 2 illustrates the types A, B, C, E.

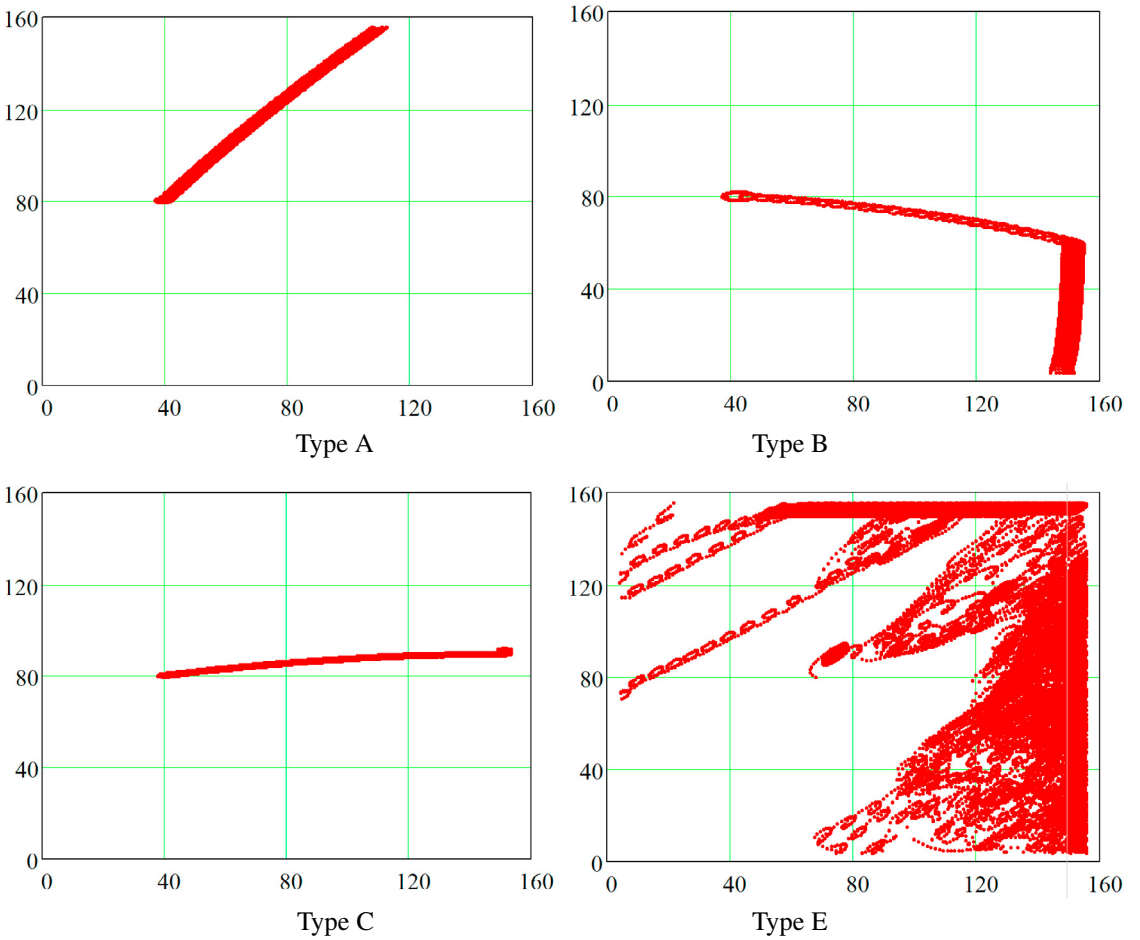

Fig. 2. Spiral wave response types. Tip(s) trajectories are shown

3.1. Results on APsimple Model

We used one stimulation electrode placed at the left bottom corner. The response types of the spiral wave are presented in Tables 4 (horizontal fibres) and 5 (diagonal fibres).

Table 4. Type of spiral wave response to external stimulation in the APsimple model, $\phi = 0$

a	Relative period of external stimulation						
	0.7	0.75	0.8	0.85	0.9	0.95	1.00
0.03	B	A	C	A	A	B	D
0.04	A	A	A	A	C	B	D
0.05	A	A1	A	A	C	C	D
0.06	A	A	A	C	C	C	D
0.07	A	B	B	A	A	B	D
0.08	B	B	B	B	B	B	D
0.09	A	A	B	B	B	B	D
0.10	A	A	A	A	A	A	A

Table 5. Type of spiral wave response to external stimulation in the APsimple model, $\phi = \pi/4$

a	Relative period of external stimulation						
	0.7	0.75	0.8	0.85	0.9	0.95	1.00
0.03	A	A	A	A2	A	A	D
0.04	A	A	A	A	A	A	D
0.05	A	A	A	A	C	C	D
0.06	A	A	A	A3	A	D	D
0.07	B	A	A	A	A	D	D
0.08	A	A	A	A	D	D	D
0.09	A	A	A	D	D	D	D
0.10	A	A	A	A	A	A	A

From both tables, we see that the external stimulation was effective in all cases for the model with $a = 0.1$ as the spiral drifted to the boundary and disappeared (type A). Stimulation with a relative period 1.00 had no effect on the spiral wave drift in all the cases with $a < 0.1$. Also, there were no cases with break-up (type E). The minimal attempted stimulation period 0.7 was, every time, still effective.

We also measured times when the spiral started to drift (T_1) and when it approached the square boundary (T_2). We saw that the time T_1 increased when the stimulation period increased, and T_1 grew when the model parameter a decreased. If the stimulation period was constant, the time T_2 was maximal at a middle value of a (0.6 or 0.7 depending on the period) and sufficiently less for $a = 0.1$. And if the parameter a was constant, the time T_2 rose with an increase of the stimulation period.

Table 5 shows an area of ineffective stimulation (type D) for higher stimulation periods (0.85 and more) and $0.06 \leq a \leq 0.09$. For $a < 0.1$, times T_1 and T_2 increased when the stimulation period increased, as for $\phi = 0$. For $a = 0.1$, T_1 was minimal for stimulation period 0.8 and T_2 was maximal for the period 0.75.

Sometimes, new spiral waves arose (types A1, A2, A3).

3.2. Results on APmu Model

We tried five configurations of electrode size, number and location:

1) one point electrode at the left bottom square corner;
2) one point electrode at the centre of the square;
3) two point electrodes at the adjacent left corners;
4) two point electrodes at the centres of the top and bottom edges;
5) long line electrode occupying the entire left edge of the square.

The results are displayed in Tables 6–8.

Comparison of our results for one-electrode cases 1 and 2 shows that an increase of the stimulation period causes a growth of the times T_1 and T_2 for all the cases except configuration 2 with $\phi = 0$. With that special case, the times oscillated and we could see no clear tendency. Also, that case is characterized by shorter times of spiral's drift (T_1

was between 200 and 300 MU and T_2 was between 680 and 1000 MU whereas T_1 was between 600 and 4400 MU and T_2 was between 800 and 5400 MU for the configuration 1, both ϕ, and configuration 2, $\phi = \pi/4$). We saw that effective stimulation periods lay on the segment $[0.8, 0.95]$. Near the left limit of this segment, break-up occurred, and near its right limit, the superseding time increases. So, the most effective and safe stimulation period should be chosen somewhere close to the segment's middle. Effect of the fibre angle is that the times $T_{1,2}$ were slightly less for $\phi = 0$ than for $\phi = \pi/4$ in configuration 1.

Let us now analyze the two-electrode configurations 3 and 4. The segment of effective superseding was the same ($[0.8, 0.95]$) for all four cases except one case, namely configuration 4, $\phi = \pi/4$, where period 0.8 was ineffective and the segment was $[0.85, 0.95]$. As in the one-electrode cases, the left limit of the segment was associated with break-up (except the same case with configuration 4, $\phi = \pi/4$) and near the right limit, the times $T_{1,2}$ grew. In most of the cases, the time of drift to the boundary was less for $\phi = \pi/4$ than for $\phi = 0$.

In general, the time needed to supersede the spiral to the boundary for one- and two-electrode configurations is nearly the same. Only the case with one electrode near the spiral core, $\phi = 0$ showed essentially shorter times.

Long-electrode configuration (5) was associated with more additional spiral waves, which arose due to more intersection points of the stimulation forefront and spiral wave backfronts. The segment of effective periods was the same, $[0.8, 0.95]$ for $\phi = \pi/4$ and even broader, $[0.8, 1.0]$ for $\phi = 0$. Time of spiral wave drift was bigger for $\phi = \pi/4$ than for $\phi = 0$. Again, low stimulation periods 0.7 and 0.75 caused break-up.

Table 6. Spiral wave response types for the APmu model

Relative stimulation period	Electrode configuration					Electrode configuration				
	1	2	3	4	5	1	2	3	4	5
	$\phi = 0$					$\phi = \pi/4$				
0.7	D	D	D	D	E	E	D5	E	D	E
0.75	E	E	E	E	E	E	E	E	D	E
0.8	A	A7	A	A	A9	AB	A4	AB	D	AB3
0.85	A	A2	A	A	A4	AB	A2	AB	C	AB2
0.9	A	A	A	C	A6	AB	A	AB	C1	AB2
0.95	C	A	A	C	C4	A	A	A	A	AB2
1.0	D	D	D	D	B9	D	Dn	D	D	D

Table 7. Time when the spiral began its drift

Relative stimulation period	Electrode configuration					Electrode configuration				
	1	2	3	4	5	1	2	3	4	5
	$\phi = 0$					$\phi = \pi/4$				
0.8	1222	250	1144	1120	491	649	361	660	—	590
0.85	1515	226	1400	1369	675	941	326	939	1097	867
0.9	2296	293	2137	2067	806	1318	553	1321	1603	1121
0.95	4144	238	3810	3681	1500	4376	725	4400	5413	3831
1.0	—	—	—	—	4906	—	—	—	—	—

Table 8. Time when the spiral drifted to the square's boundary

Relative stimulation period	Electrode configuration					Electrode configuration				
	1	2	3	4	5	1	2	3	4	5
	$\phi = 0$					$\phi = \pi/4$				
0.8	1396	943	1185	2849	634	835	653	831	—	806
0.85	1679	680	1473	2997	845	1156	473	1157	1393	1133
0.9	2481	970	2222	2800	1051	1633	750	1633	2008	1613
0.95	4354	464	3927	3900	1948	5378	1465	5377	5728	4593
1.0	—	—	—	—	5508	—	—	—	—	—

A comparison of three configurations 1, 3, and 5, where electrode(s) were placed only at the left edge of the square, shows that times $T_{1,2}$ are close in all the cases except configuration 5, $\phi = 0$, where the times are significantly shorter (1500–2000 MU vs. 4000–5000 MU).

4. Discussion and Conclusions

Previously we performed similar simulations for isotropic cardiac tissue [14]. Comparison of the results for the isotropic and anisotropic cases reveals that similar drift regimes (A, B, C, D) can be observed. Quantitatively, the time moments of drift begin and end $T_{1,2}$ were smaller in the anisotropy than in the isotropy for electrode configurations 1, 3 (both for $\phi = \pi/4$) and 5; they were larger in anisotropy for cases 3 ($\phi = \pi/4$) and 4; the times were similar in case 1, $\phi = 0$; finally, for case 2, no studies for isotropy were performed. Because, mathematically, the anisotropy with parallel fibres is equivalent to rescaling in certain directions, the observed differences can be explained by change in the effective geometry, size and location of the boundaries of the domain.

Calculations on isotropic models of the myocardium with the APsimple model [14] show that the external stimulation is effective if its relative period is less than some upper limit (about 0.98) but the precise value of the lower limit has not been found there. Here, we continued the work and explored periods from 0.7 for the anisotropic case. We found that stimulation is still effective at periods as low as 0.7.

Cardiac tissue model APmu with the parameters we used is considered to more accurately represent myocardial properties. Qualitatively, our results for the anisotropy are similar to those for the isotropy [14]. The effective stimulation periods are between 0.8 and 0.95. The shortest stimulation period results in the minimal superseding time but is dangerous due to the risk of breakup. The larger the period is, the more time to move the spiral to the boundary is necessary.

Experimental studies of effects of high-frequency simulation on spiral waves were performed in the BZ chemical reaction [8]. It was shown that such stimulation can result in an induced drift of spiral waves, and the drift speed increases with a decrease in the stimulation period. The drift pattern described in [8] corresponds well to the regime obtained for wave trains in our stimulation configuration 5 in APmu model. Although we did not measure drift speed directly, the overall time intervals between the beginning and end of the drift in our simulations show the drift speed also increases with a decrease in the stimulation period.

In the anisotropic models, sometimes new spiral waves appeared, which was not observed in isotropic AP-based simulations in [14]. At the same time, appearance and effect of new spirals are key for LVD in TP06 simulations since cardioversion is achieved there not by superseding, but by annihilation of the ”original” spiral with a new spiral. We observed two ways how new spirals can appear. They are illustrated in Fig. 2E. First, stimulation from the electrode can occur at the waveback of an existing wave so it initiates new spirals, as in the well-known S1S2 protocol [7]. Second, we observed formation of new spirals at some distance from the electrode close to the core of the existing spiral wave, or at the boundary. The new spirals were formed due to interaction between plane waves produced by the electrode and the original spiral wave.

One of the limitations of our study is that we used simple phenomenological cell models that do not include ionic currents. One of these models is TP06, which has 18 phase variables. Simulation of such a model is computationally intensive and requires more computing resources than AP models thus it needs to develop more sophisticated algorithms which use not only OpenMP but MPI, or even automated scientific computing libraries.

In future work, we are going to consider ionic cell-level models, which describe action potentials in the cardiac cells more accurately. The electrode in one of the analyzed configurations was placed near the spiral core, and an interesting direction of future work is a study of the case when an electrode is inside the core, as was done in [22] for a model of some excitable chemical 2D isotropic medium. Also, as it is known that mechano-electrical feedback causes drift of spiral waves toward the boundaries, heart models with mechanics will be studied. Practical implementation of such research is impossible without realistic 3D simulations, so we plan to generalize our work on 3D models of the left ventricle, for example, as proposed in [15, 13].

Acknowledgements

Our work is supported by an RSF project 17-71-20024 (IMM UB RAS).

References

[1] R.R. Aliev and A.V. Panfilov. A simple two-variable model of cardiac excitation. *Chaos, Solitons and Fractals*, 7(3):293–301, 1996.

[2] Bryan J. Caldwell, Mark L. Trew, and Arkady M. Pertsov. Cardiac response to low-energy field pacing challenges the standard theory of defibrillation. *Circulation: Arrhythmia and Electrophysiology*, 8(3):685–693, 2015.

[3] E.A. Ermakova, V.I. Krinsky, A.V. Panfilov, and A.M. Pertsov. Interaction between spiral and flat periodic autowaves in an active medium. *Biofizika*, 31(2):318–323, 1986. In Russian.

[4] Flavio Fenton and Alain Karma. Vortex dynamics in three-dimensional continuous myocardium with fiber rotation: Filament instability and fibrillation. *Chaos: An Interdisciplinary Journal of Nonlinear Science*, 8(1):20–47, 1998.

[5] Georg Gottwald, Alain Pumir, and Valentin Krinsky. Spiral wave drift induced by stimulating wave trains. *Chaos: An Interdisciplinary Journal of Nonlinear Science*, 11(3):487–494, 2001.

[6] D. Hornung, V. N. Biktashev, N. F. Otani, T. K. Shajahan, T. Baig, S. Berg, S. Han, V. I. Krinsky, and S. Luther. Mechanisms of vortices termination in the cardiac muscle. *Royal Society Open Science*, 4(3), 2017.

[7] R. H. Keldermann, K. H. W. J. ten Tusscher, M. P. Nash, R. Hren, P. Taggart, and A. V. Panfilov. Effect of heterogeneous apd restitution on vf organization in a model of the human ventricles. *American Journal of Physiology - Heart and Circulatory Physiology*, 294(2):H764–H774, 2008.

[8] V.I. Krinsky and K.I. Agladze. Interaction of rotating waves in an active chemical medium. *Physica D: Nonlinear Phenomena*, 8(1):50 – 56, 1983.

[9] Stefan Luther, Flavio H. Fenton, Bruce G. Kornreich, et al. Low-energy control of electrical turbulence in the heart. *Nature*, 475:235–239, 2011.

[10] Kazuo Nakazawa et al. *Computational Analysis and Visualization of Spiral Wave Reentry in a Virtual Heart Model*, pages 217–241. Springer Tokyo, 2000.

[11] Martyn P. Nash and Alexander V. Panfilov. Electromechanical model of excitable tissue to study reentrant cardiac arrhythmias. *Progress in Biophysics and Molecular Biology*, 85(2):501 – 522, 2004. Modelling Cellular and Tissue Function.

[12] A.V. Panfilov and J.P. Keener. Effects of high frequency stimulation in excitable medium with obstacle. *J.Theor. Biol.*, 163:439–448, 1993.

[13] Sergei Pravdin. A mathematical spline-based model of cardiac left ventricle anatomy and morphology. *Computation*, 4 (4)(42), 2016.

[14] Sergei F. Pravdin, Timur V. Nezlobinsky, and Alexander V. Panfilov. Inducing drift of spiral waves in 2D isotropic model of myocardium by means of an external stimulation. In *MPMA-2017 Proceedings, CEUR-WS*, volume 1894, pages 268–284.

[15] S.F. Pravdin, V.I. Berdyshev, A.V. Panfilov, L.B. Katsnelson, O. Solovyova, and V.S. Markhasin. Mathematical model of the anatomy and fibre orientation field of the left ventricle of the heart. *Biomedical Engineering Online*, 54(12), 2013.

[16] S. Sinha and S. Sridhar. *Patterns in Excitable Media: Genesis, Dynamics, and Control*. Taylor & Francis, 2014.

[17] Michael O. Sweeney. Antitachycardia pacing for ventricular tachycardia using implantable cardioverter defibrillators:. *Pacing and Clinical Electrophysiology*, 27(9):1292–1305, 2004.

[18] Kirsten HWJ Ten Tusscher and Alexander V Panfilov. Alternans and spiral breakup in a human ventricular tissue model. *American Journal of Physiology-Heart and Circulatory Physiology*, 291(3):1088–1100, 2006.

[19] Mark S. Wathen, Paul J. DeGroot, Michael O. Sweeney, et al. Prospective randomized multicenter trial of empirical antitachycardia pacing versus shocks for spontaneous rapid ventricular tachycardia in patients with implantable cardioverter-defibrillators. *Circulation*, 110(17):2591–2596, 2004.

[20] Dan Wilson and Jeff Moehlis. An energy-optimal methodology for synchronization of excitable media. *SIAM Journal on Applied Dynamical Systems*, 13(2):944–957, 2014.

[21] Dan Wilson and Jeff Moehlis. Toward a more efficient implementation of antifibrillation pacing. *PLOS ONE*, 11(7):1–28, 07 2016.

[22] Hong Zhang, Bambi Hu, and Gang Hu. Suppression of spiral waves and spatiotemporal chaos by generating target waves in excitable media. *Phys. Rev. E*, 68:026134, Aug 2003.